

**Short Note**

**Approximating edges of source bodies from magnetic or gravity anomalies**

Richard J. Blakely\* and Robert W. Simpson\*

**INTRODUCTION**

Cordell and Grauch (1982, 1985) discussed a technique to estimate the location of abrupt lateral changes in magnetization or mass density of upper crustal rocks. The final step of their procedure is to identify maxima on a contoured map of horizontal gradient magnitudes. We attempt to automate their final step. Our method begins with gridded magnetic or gravity anomaly data and produces a plan view of inferred boundaries of magnetic or gravity sources. The method applies to both local surveys and to continent-wide compilations of magnetic and gravity data (e.g., Zietz, 1982; Simpson et al., 1983a; Kane et al., 1982).

**METHOD**

Cordell and Grauch (1982, 1985) described a three-step procedure for locating edges of magnetic bodies. First, the pseudogravity transform (Baranov, 1957) is applied to the magnetic data. The pseudogravity transform is a linear filter, usually applied in the Fourier domain, that transforms the magnetic anomaly observed over a magnetization distribution  $m(x, y, z)$  into the gravity anomaly that would be observed if density  $\rho(x, y, z) = km(x, y, z)$ , where  $k$  is a constant. Second, the magnitude of the horizontal gradient of the pseudogravity anomaly is calculated. Because shallow bodies produce gravity anomalies with maximum horizontal gradients located nearly over their edges, the two steps transform magnetic anomalies into ridges of maximum pseudogravity gradients that may overlie the edges of causative magnetic bodies. Third, a contour map of the maximum horizontal gradient is visually inspected for the locations and significance of linear maxima. For application of the method to gravity data, only the final two steps are required (Cordell, 1979).

We automated the final step of the Cordell-Grauch procedure to provide objective and rapid interpretation of horizontal gradient magnitudes. Because of the prior processing steps, the horizontal gradient data are available on a rectangular grid. Each grid intersection  $g_{i,j}$  (except the marginal rows and columns) is compared with its eight nearest neighbors in four directions (along the row, column, and both diag-

onals) to see if a maximum is present (Figure 1). This comparison tests the following inequalities:

$$g_{i-1,j} < g_{i,j} > g_{i+1,j},$$

$$g_{i,j-1} < g_{i,j} > g_{i,j+1},$$

$$g_{i+1,j-1} < g_{i,j} > g_{i-1,j+1},$$

and

$$g_{i-1,j-1} < g_{i,j} > g_{i+1,j+1}.$$

A counter  $N$  is increased by one for each satisfied inequality. Hence,  $N$  ranges from 0 to 4 and provides a measure of the "quality" of the maximum; we shall refer to the parameter  $N$  as the "significance level" of the maximum.

For each satisfied inequality, the horizontal location and magnitude of the maximum are found by interpolating a second-order polynomial through the trio of points. For example if

$$g_{i-1,j} < g_{i,j} > g_{i+1,j},$$

the horizontal location of the maximum relative to the position of  $g_{i,j}$  is given by

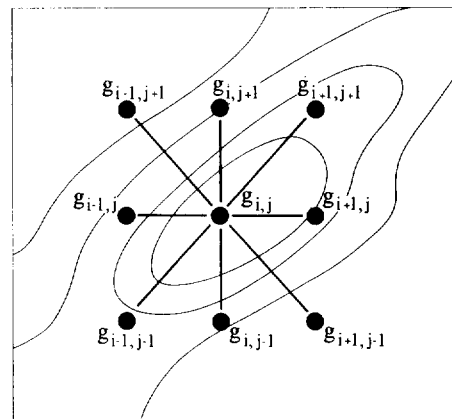


FIG. 1. Location of grid intersections used to test for a maximum near  $g_{i,j}$ . Curved lines represent contours of horizontal gradient values of magnetic or gravity anomalies.

Manuscript received by the Editor April 15, 1985; revised manuscript received December 26, 1985.

\*U.S. Geological Survey, 345 Middlefield Road, Menlo Park, CA 94025. This paper was prepared by an agency of the U.S. government.

$$x_{\max} = -\frac{bd}{2a},$$

where

$$a = \frac{1}{2}(g_{i-1,j} - 2g_{i,j} + g_{i+1,j}),$$

$$b = \frac{1}{2}(g_{i+1,j} - g_{i-1,j}),$$

and  $d$  is the distance between grid intersections. The value of the horizontal gradient at  $x_{\max}$  is given by

$$g_{\max} = ax_{\max}^2 + bx_{\max} + g_{i,j}.$$

If more than one inequality is satisfied, the largest  $g_{\max}$  and its corresponding  $x_{\max}$  are chosen as the appropriate maxima for that grid intersection.

A record of  $x_{\max}$ ,  $g_{\max}$ , and  $N$  is kept for each grid intersection where  $N > 0$ . The user can display maxima in geodetic coordinates at any of the four significance levels. We have found that  $N = 2$  or 3 produces the most useful maps. In general,  $N = 1$  analyses are too loosely constrained to provide meaningful information. For example, maxima may appear to radiate from symmetric anomalies with directions that depend upon the orientation of the grid with respect to the anomaly. In some surveys, maxima may be so prevalent that some of the smaller and perhaps less significant values of  $g_{\max}$  must be discarded. Hence, the method permits the user to specify a tolerance level  $g_{\text{tol}}$  such that only  $g_{\max} > g_{\text{tol}}$  will be displayed.

Note that this analysis requires no assumptions about the sources except, in the magnetic case, the direction of magnetization. Maxima will nearly overlie edges of shallow sources with abrupt and near-vertical contacts. Nonvertical contacts will generally result in calculated boundaries that less precisely mark the surface trace of the contacts. Note that certain classes of bodies produce anomaly gradients that bear no relation to the body's lateral extent. The gravity, or pseudogravity, anomaly over a spherical source, for example, has maximum horizontal gradients in the shape of a circular ring, but the diameter of the ring depends only on the depth to the center of the sphere and provides no independent information about the size of the sphere. Also, topographic features in magnetic terrane have abrupt magnetic boundaries (with air). The boundary analysis should be used with caution in areas of significant topographic relief.

#### TEST CASES

Figure 2 shows results when the method was applied to the magnetic anomaly over a buried rectangular prism. The prism has horizontal dimensions of 10 km, thickness of 3 km, and direction of magnetization with inclination  $60^\circ\text{E}$  and declination  $15^\circ\text{E}$ . The anomaly was calculated on a level surface 4 km above the top surface of the prism. Sample intervals were 0.5 km to both the east and north. The only information required by the boundary analysis is the grid of anomaly values and the inclination and declination of magnetization.

The calculated boundaries are shown in plan view for  $N = 3$ . The method correctly predicts the size and shape of the magnetic boundary, but it tends to round the corners. The rounded corners are not a consequence of a large grid interval; we repeated this test with a sample interval of 0.25 km, for example, and the calculated shape was identical to that in Figure 2. Abrupt corners of a source contain, in a sense, the shortest wavelengths of  $m(x, y, z)$ . Hence, in a magnetic or

gravity anomaly measured some distance away, information about source corners is more attenuated than other attributes about the shape of the source.

We tested the method on a variety of prism configurations. For shallower sources, the calculated plan-view shape closely approaches the correct shape of the prism. For deeper sources, the calculated boundary becomes more rounded and ultimately approaches a circular shape that expands as depth increases.

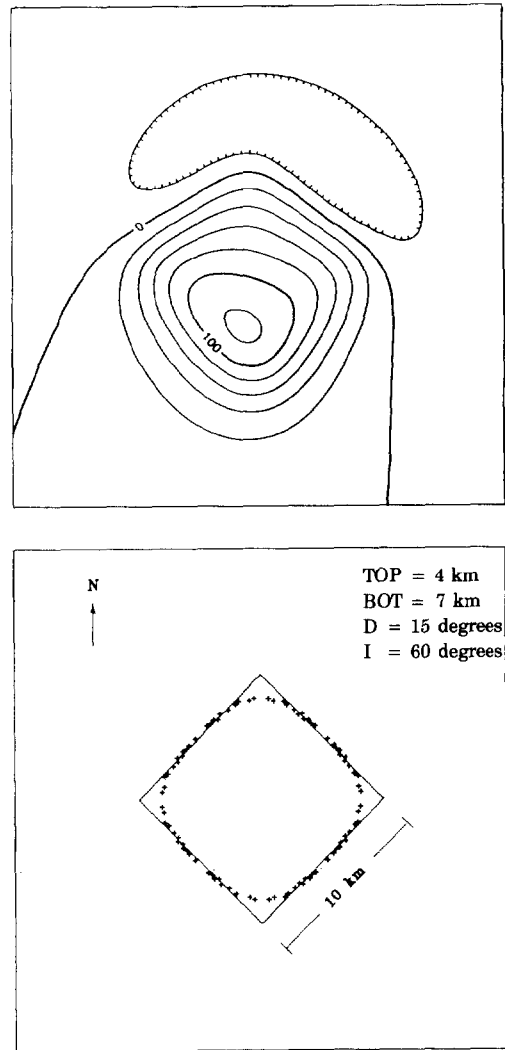


FIG. 2. Test of the boundary analysis technique. Upper map represents the calculated total field anomaly over a prism with horizontal dimension of 10 km, vertical dimension of 3 km, and buried 4 km below the level of measurement. Sample intervals are 0.25 km in both the north and east directions. Inclination and declination of magnetization and regional field are  $60^\circ\text{E}$  below the horizon and  $15^\circ\text{E}$ , respectively. Intensity of magnetization is 10 A/m. Contour interval is 20 nT. Hachures indicate closed lows. Bottom map shows the true boundaries in plan view of the prism (solid line) and the locations of maximum horizontal gradients (plus symbols). Top and bottom maps are at same scale and orientation.

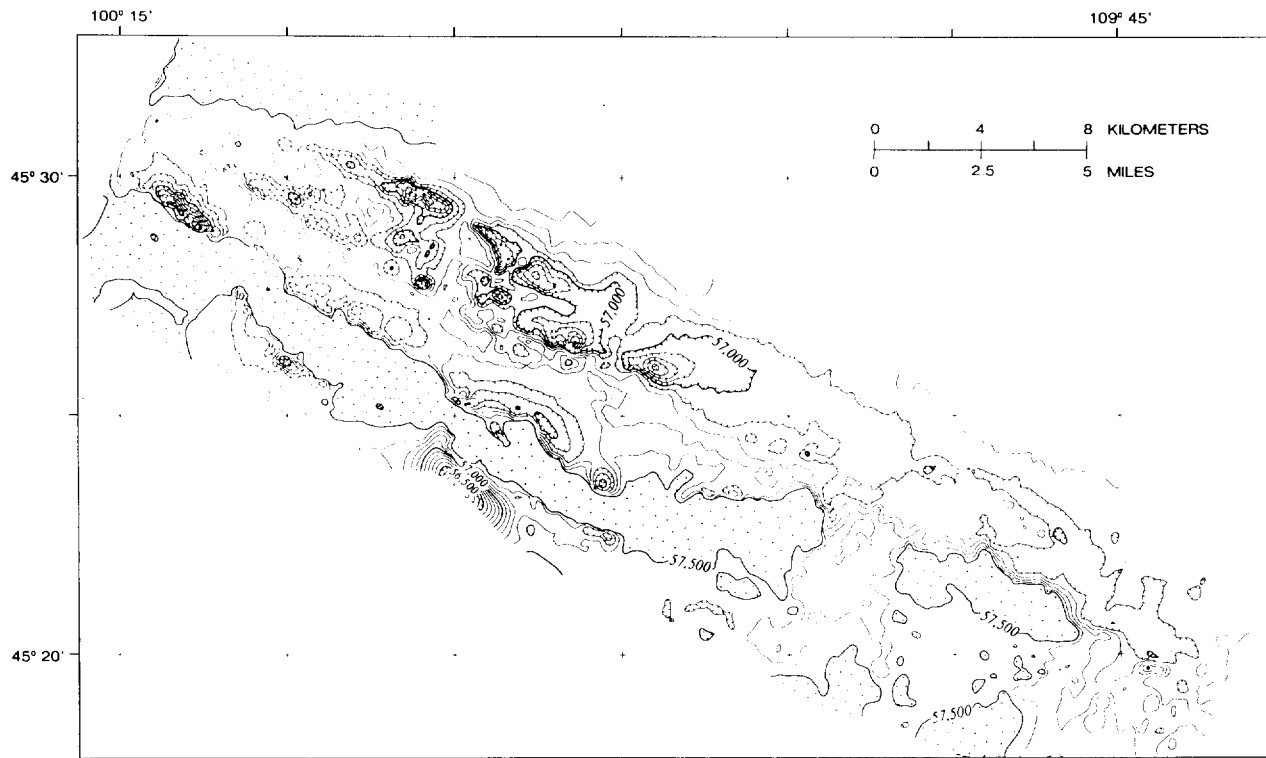


FIG. 3. Aeromagnetic data over the Stillwater complex of south-central Montana recorded by Anaconda Minerals Company. Contour interval 100 nT for magnetic intensities less than 57 500 nT. Stipple areas without contours indicate magnetic intensities exceeding 57 500 nT. Hachures indicate closed lows.

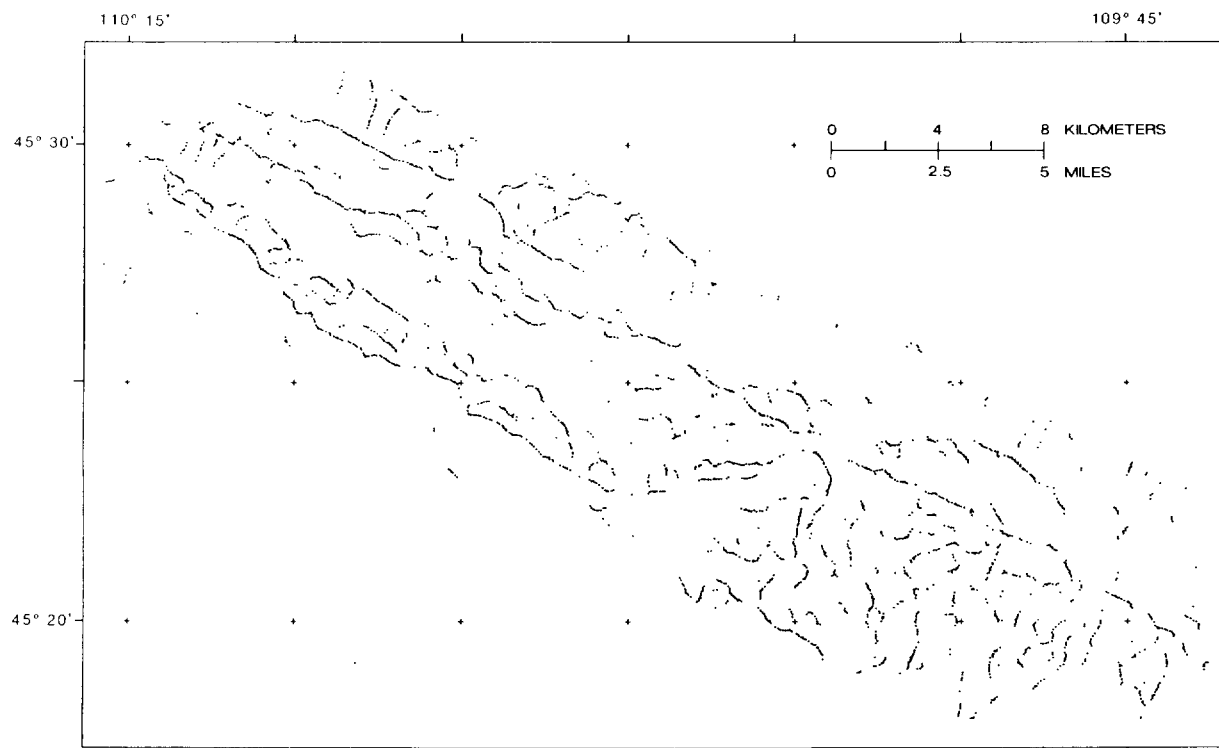


FIG. 4. Location of magnetic boundaries within the Stillwater complex and adjacent rocks, Montana. Calculated from aeromagnetic data of Figure 3.

### MAGNETIC EXAMPLE FROM THE STILLWATER COMPLEX

The following example demonstrates the method as applied to a magnetic survey over the Stillwater complex, a stratiform mafic intrusion of Archean age in south-central Montana (Page, 1977). The aeromagnetic survey (Figure 3) was flown by Anaconda Minerals Company in 1978 along flight lines spaced at approximately 260 m and directed north-northeast, roughly normal to the main geologic features of the complex. Data were collected by helicopter at a mean terrain clearance of 76 m. Blakely and Zientek (1985) discussed the data and their geologic implications. The aeromagnetic data show a number of magnetic anomalies lineated generally parallel to the banded features of the Stillwater complex. The anomalies with greatest amplitude exceed 6 000 nT, are located in the uncounted stipple areas in Figure 3, and occur over the iron formation within the metamorphic aureole below the base of the complex; less intense anomalies are produced by the ultramafic series (or zone) and the banded series (or zone) within the complex.

Figure 4 shows the results of the boundary analysis applied to the aeromagnetic data of Figure 3. The sinuous sequences of dots in Figure 4 represent magnetic boundaries (assuming the boundaries are abrupt and vertical). Blakely and Zientek (1985) used this boundary analysis to calculate magnetization contrasts inside and outside the complex. The original data (Figure 3) are difficult to interpret (and to contour) because of

the extreme range of magnetic intensities. The boundary analysis in Figure 4, however, makes interpretation much more straightforward. It would, of course, be unwise to interpret all maxima in Figure 3 as authentic source boundaries; each should be carefully compared with the original aeromagnetic map. Any features on the boundary map not evident on the anomaly map should be regarded with caution.

### APPLICATION TO GRAVITY IN THE UNITED STATES

Figure 5 shows the boundary analysis applied to the isostatic residual gravity of the conterminous United States. Simpson et al. (1983b) computed isostatic residual gravity anomalies by assuming isostatic compensation of topographic loads according to an Airy-Heiskanen model (Simpson, Jachens, and Blakely, 1983) and subtracting the gravitational effect of the compensating masses from the gridded Bouguer anomaly data developed by Godson and Scheibe (1982). The long-wavelength effects of deep, compensating sources are thereby eliminated (at least to first order), and the isostatic residual map indicates mostly lateral variations of density within the crust.

Figure 5 shows the location of maxima with  $N = 3$  and  $g_{\max} > 1.5$  mGal/km. The sinuous sequences of maxima represent the major horizontal gradients of the residual gravity field of the United States. Many of these gradients can be attributed to geologic bodies and major structures of the United States (e.g., Simpson et al., 1983b; Kane et al., 1982). Note, for

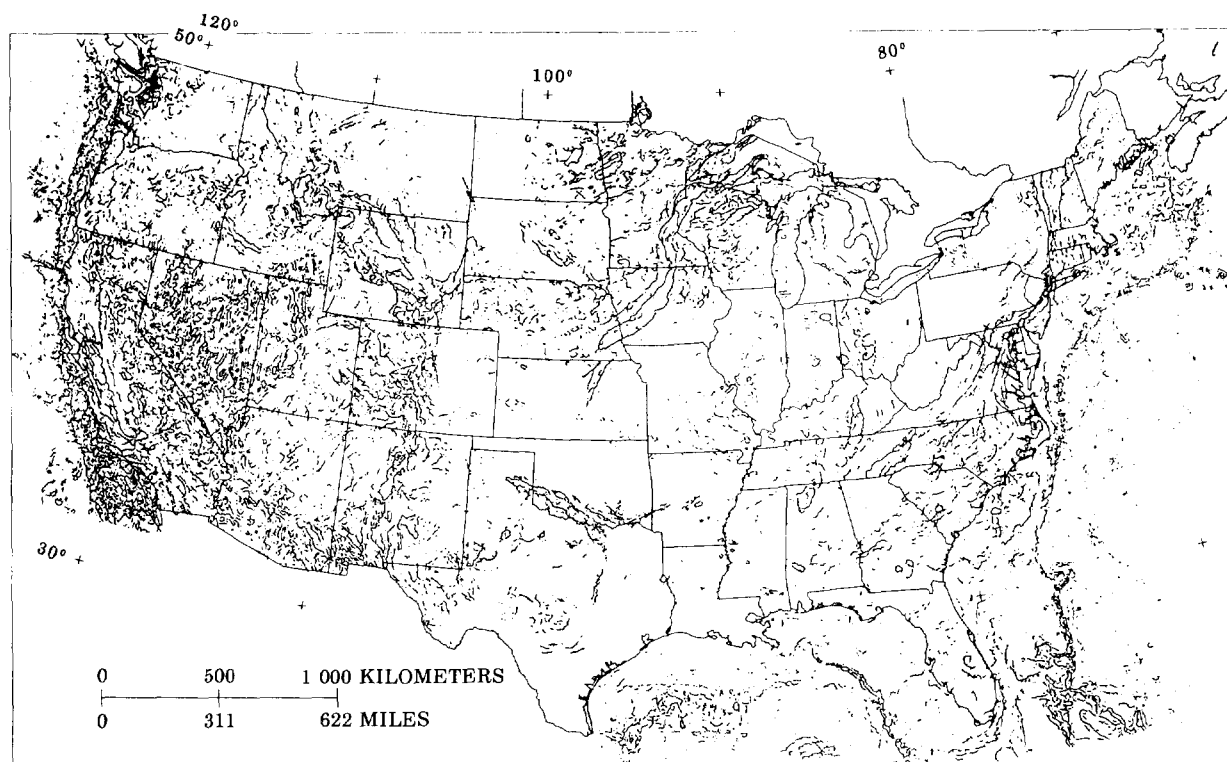


FIG. 5. Map showing location of maxima in the horizontal gradient of the isostatic residual gravity anomaly data for the United States (Simpson et al, 1983b). Only maxima exceeding 1.5 mGal/km are shown.

example, the boundaries associated with the Snake River Plateau in southwestern Idaho, the Laramide orogenies in Wyoming, and the Precambrian rift system in Iowa and neighboring states.

### CONCLUSIONS

We have found that the pseudogravity transformation followed by a horizontal gradient calculation, as discussed in Cordell (1979) and Cordell and Grauch (1982, 1985), is a useful method to aid interpretation of magnetic data, and that automatic location of maximum horizontal gradients is a useful extension of this technique. We emphasize that this technique is simply a tool to aid interpretation, and that it remains the job of the interpreter to decide on the geologic reality of the results. Geologic features that appear in the boundary analysis are always present and detectable (at least with hindsight) in the original magnetic or gravity data, but the analysis helps guide the interpreter to features and patterns that might not otherwise have been readily detected in the original data.

The method is programmed in standard Fortran and is available on magnetic tape in ANSI format. Send a blank magnetic tape to the authors with requests for copies of the program.

### ACKNOWLEDGMENTS

We thank Anaconda Minerals Company for providing us with and allowing us to publish the aeromagnetic data shown in Figure 3.

### REFERENCES

- Baranov, V., 1957, A new method for interpretation of aeromagnetic maps: Pseudo-gravimetric anomalies: *Geophysics*, **22**, 359-383.
- Blakely, R. J., and Zientek, M. L., 1985, Magnetic anomalies over a mafic intrusion: The Stillwater complex, in Czamanske, G. K., and Zientek, M. L., Eds., *The Stillwater complex, Montana: Geology and guide*: Montana Bureau of Mines and Geol., Spec. Pub. **92**, 39-45.
- Cordell, L., 1979, Gravimetric expression of graben faulting in Santa Fe country and the Española basin, New Mexico, in Ingersoll, R. V., Ed., *Guidebook to Santa Fe country*: New Mexico Geol. Soc. Guidebook, 30th Field Conference, 59-64.
- Cordell, L., and Grauch, V. J. S., 1982, Mapping basement magnetization zones from aeromagnetic data in the San Juan Basin; New Mexico: Presented at the 52nd Ann. Internat. Mtg., Soc. Explor. Geophys., Dallas; abstracts and biographies, 246-247.
- 1985, Mapping basement magnetization zones from aeromagnetic data in the San Juan basin, New Mexico, in Hinze, W. J., Ed., *The utility of regional gravity and magnetic anomaly maps*: Soc. Explor. Geophys., 181-197.
- Godson, R. H., and Scheibe, D. M., 1982, Description of magnetic tape containing conterminous U.S. gravity data in gridded format: National Tech. Information Serv., PB82-254798 (magnetic tape with description).
- Kane, M. F., Hildenbrand, T. G., Simpson, R. W., Godson, R. H., and Bracken, R. E., 1982, Crust and mantle structure of the conterminous U.S. from wavelength-filtered gravity data: Presented at the 52nd Ann. Internat. Mtg., Soc. Explor. Geophys., Dallas; abstracts and biographies, 232-234.
- Page, N. J., 1977, Stillwater complex, Montana: rock succession, metamorphism, and structure of the complex and adjacent rocks: U.S. Geol. Surv. Prof. Paper 999.
- Simpson, R. W., Jachens, R. C., and Blakely, R. J., 1983, AIRY-ROOT: A FORTRAN program for calculating the gravitational attraction of an Airy isostatic root out to 166.7 km: U.S. Geol. Surv. open-file rep. 83-883.
- Simpson, R. W., Jachens, R. C., Saltus, R. W., and Godson, R. H., 1983a, Airy isostatic residual gravity map of the conterminous United States: *Trans., Am. Geophys. Union*, **64**, 863.
- 1983b, A description of colored isostatic gravity maps and a topographic map of the conterminous United States available as 35 mm slides: U.S. Geol. Surv. open-file rep. 83-884.
- Zietz, I., 1982, Composite magnetic anomaly map of the United States—Part A: conterminous United States: U.S. Geol. Surv., Geophys. Invest. Map GP-954-A, scale 1 : 2 500 000.